

Validation of a nonlinear spectral model for water waves over a variable bathymetry

M. Gouin^{1,2}, G. Ducrozet¹, and P. Ferrant¹

¹Ecole Centrale Nantes, LHEEA Lab., UMR CNRS 6598, Nantes, France

²Institut de Recherche Technologique Jules Verne, Bouguenais, France

*maite.gouin@ec-nantes.fr

Highlights

- Presentation of an HOS scheme for modelling non-linear water waves over a variable bathymetry.
- Validation of the method for a small variation of the bottom with Bragg reflection.
- Application of the HOS model to wave propagation over a bathymetry with high variation of the bottom: submerged bar.

Introduction

The accurate modelling of surface gravity waves over non-negligible bottom topography is of major interest in the field of marine renewable energy. These marine renewable structures are intended to be located in limited water depth, where the effect of variable bathymetry is very significant on local wave conditions. Indeed, when entering shallow water, waves are strongly affected by the bottom through shoaling, refraction, diffraction, reflection and the resulting variations in local wave speed.

In [8] two different schemes for modelling a bathymetry with a High-Order Spectral (HOS) method have already been presented. This highly non-linear potential model has been initially developed [16, 5] for a flat bottom and extensively validated for different configurations in the LHEEA Lab [7, 6] from regular waves up to irregular multidirectional wavefields. This model, named HOS-ocean is available as an open-source version¹. In the present paper, we focus on the efficient scheme allowing the use of FFTs presented in [8].

A few HOS applications consider a variable bathymetry. Liu and Yue [10] provided one simulation case with a bottom variation using the HOS method, but considering only a small variation of the bottom. This case reproduces Class I Bragg reflection and will be presented here as a validation of our model. The second case presented in this paper is more extreme with large bottom variations. Nevertheless, our method shows good results which are compared both to experimental results [11, 4] and numerical results obtained with other methods [1, 9].

Methods and Algorithms

Hypothesis and formulation of the problem

In this section, the main hypothesis and equations are presented briefly. More details are available in [8].

$z = \eta(x, t)$ represents the free surface elevation, h the total water depth, h_0 the mean depth and $\beta(x)$ the bottom variation, such as $-h(x) = -h_0 + \beta(x)$. Thus we have : $-h_0 + \beta(x) \leq z < \eta(x)$. A potential flow formalism is used (incompressible and inviscid fluid, irrotational flow) and we assume periodic boundary conditions in the horizontal plane so that the domain is considered infinite. We obtain the following set of equations:

- Laplace equation in the fluid domain:

$$\Delta\phi = 0 \quad (1)$$

- Free-surface boundary conditions (FSBC) written in terms of surface quantities η and $\tilde{\phi}$ ($\tilde{\phi}(x, t) = \phi(x, z = \eta, t)$):

$$\frac{\partial\eta}{\partial t} = \left(1 + \left|\frac{\partial\eta}{\partial x}\right|^2\right) \frac{\partial\phi}{\partial z} - \frac{\partial\tilde{\phi}}{\partial x} \cdot \frac{\partial\eta}{\partial x} \quad \text{on } z = \eta(x, t) \quad (2)$$

$$\frac{\partial\tilde{\phi}}{\partial t} = -g\eta - \frac{1}{2} \left|\frac{\partial\tilde{\phi}}{\partial x}\right|^2 + \frac{1}{2} \left(1 + \left|\frac{\partial\eta}{\partial x}\right|^2\right) \left(\frac{\partial\phi}{\partial z}\right)^2 \quad \text{on } z = \eta(x, t) \quad (3)$$

- Bottom boundary condition (BBC):

$$\frac{\partial\phi}{\partial x} \frac{\partial\beta}{\partial x} - \frac{\partial\phi}{\partial z} = 0 \quad \text{on } z = -h_0 + \beta(x) \quad (4)$$

To account for a bottom variation, an additional potential is introduced. The total potential ϕ_{tot} solution of the problem is expressed as:

$$\phi_{tot} = \phi_{h_0} + \phi_{\beta} \quad (5)$$

ϕ_{h_0} satisfies a Neumann condition on $z = -h_0$, therefore ϕ_{h_0} is solution of the problem at constant depth h_0 . ϕ_{β} allows the definition of the correct bottom boundary condition (Eq.4) and satisfies a Dirichlet condition on $z = 0$.

In 2D, the potentials are expanded on basis functions taking into account the previous boundary conditions:

$$\phi_{h_0}(x, z, t) = \sum_j A_j(t) \frac{\cosh(k_j(z + h_0))}{\cosh(k_j h_0)} e^{ik_j x} \quad (6)$$

¹<https://github.com/LHEEA/HOS-ocean/wiki>

$$\phi_\beta(x, z, t) = \sum_j B_j(t) \frac{\sinh(k_j z)}{\cosh(k_j h_0)} e^{ik_j x} \quad (7)$$

with $k_j = \frac{j 2\pi}{L_x}$ and $(A_j(t), B_j(t))$ the modal amplitudes of ϕ_{h_0} and ϕ_β respectively.

High-Order-Spectral Method

The HOS model is a pseudo-spectral model initially developed in [16, 5]. The potential is expressed as a truncated power series of components $\phi^{(m)}$ for $m = 0$ to M (M is the order of the HOS method). Then, the potential evaluated at the free surface is expanded in a Taylor series with respect to the mean water level $z = 0$. Combining these two expansions gives a triangular set of Dirichlet problems for the components that can be solved by means of a spectral method (allowing the use of FFT's for efficient computations). One more equation is needed to find the modal amplitudes $A_{j_1}^{(m)}(t)$ and $B_{j_1}^{(m)}(t)$ at each order m .

These are given by the iterative method described hereafter (Fig.2). Once they are computed, the vertical velocity W at the free surface can be obtained from another triangular system. The solution ϕ_{tot} is then advanced in time as described in Fig.1, with W computed as represented in Fig.2.

The bottom condition (Eq.4) reads:

$$\sum_{m=1}^M \frac{\partial \phi_{tot}^{(m)}}{\partial x} \frac{\partial \beta}{\partial x} - \sum_{m=1}^M \frac{\partial \phi_{tot}^{(m)}}{\partial z} = 0 \text{ on } z = -h_0 + \beta(x) \quad (8)$$

By assuming that $\beta \ll 1$ we can write a Taylor expansion with respect to the mean depth $z = -h_0$ at the order M . We also assume² that $O(\beta) \equiv O\left(\frac{\partial \beta}{\partial x}\right) \equiv O(\eta)$ and we keep only terms of order $\eta^{(m)}$. Thus we find the equations presented in [10]:

$$m = 1 : \frac{\partial \phi_{tot}^{(1)}}{\partial z}(x, -h_0, t) = 0$$

$$m = 2..M :$$

$$\frac{\partial \phi_{tot}^{(m)}}{\partial z}(x, -h_0, t) = \sum_{l=1}^{m-1} \frac{\partial}{\partial x} \left[\frac{\beta^l}{l!} \frac{\partial^{l-1}}{\partial z^{l-1}} \left(\frac{\partial \phi_{tot}}{\partial x} \right)^{(m-l)} \right]_{z=-h_0} \quad (9)$$

Perturbation expansions are truncated at order M . This new development Eq.(9) allows the computation of the modal amplitudes $B_{j_1}^{(m)}(t)$ at each order in function of the $A_{j_1}^{(m)}(t)$, and is independent of the position x , so FFT's can still be used, preserving the numerical efficiency of original HOS scheme as seen in [8].

Validations

In [8], a validation case has already been presented to assess the domain of applicability of our method. It allows to check the convergence of the scheme on the reconstruction of the vertical velocity with a wide variety of wave conditions and non-negligible (but constant) bottom variations. Here we present a test case to demonstrate the accuracy and efficiency of the proposed

²If Taylor expansions in η and β converge, the equality on the orders of magnitude is meaningless.

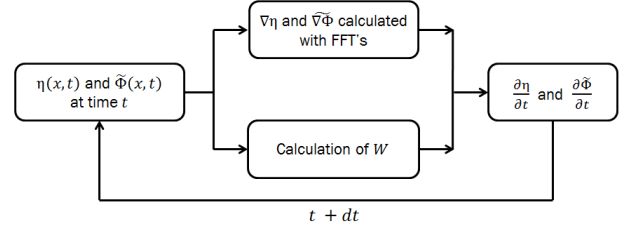


Figure 1: Temporal solution of the FSBC.

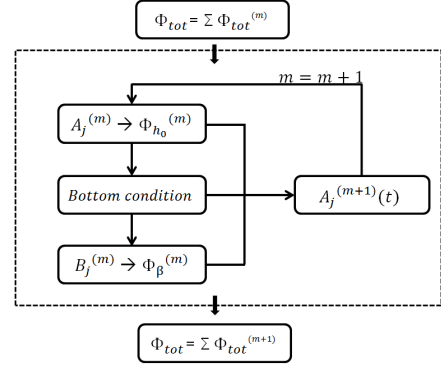


Figure 2: Use of the BBC in the temporal solution.

HOS model with a variable bathymetry. As an example of a small bottom variation, and in order to satisfy the conditions of the Taylor expansion ($\beta \ll 1$), the proposed test case considers Bragg reflection from a sinusoidal bottom patch.

Bragg reflection

If the class I Bragg condition is satisfied, the reflected wave should be amplified as a result of resonant quadratic interaction between the incident wave and the bottom variation. For small incident waves and small bottom slopes, reflection near Bragg resonances is well predicted by multiple-scale linearized perturbation theory [12]. Here we analyse non-linear effects. The conditions of the experimental set-up [3] are used to compare with their experiments.

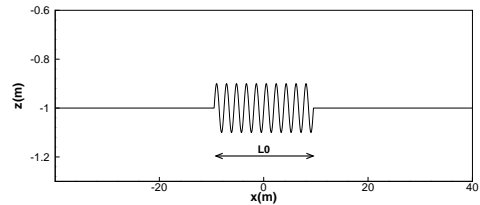


Figure 3: bottom topography with a patch of 10 sinusoidal ripples of amplitude $d = 0.1$ and slope $k_b d = 0.31$.

The bottom patch is defined as the variation around the mean water depth $h = h_0 + \beta(x)$ by :

$$\beta(x) = d \sin(k_b x) \text{ for } -L_0 \leq x \leq L_0 \quad (10)$$

as depicted in Fig.3, with k_b the bottom wavenumber. The free surface is located at $z = 0$. The ripple slope

is $k_b d = 0.31$, the ripple amplitude is $d = 0.1m$ and the length of the patch is $\frac{L_0}{\lambda_b} = 10$ (i.e. a patch of 10 sinusoidal ripples of wavelength $\lambda_b = \frac{2\pi}{k_b}$). The incident wave is at the linear resonance condition of $k = \frac{k_b}{2}$ with a wave steepness of $ka = 0.05$. In order to ensure periodicity relaxation zones are used to impose the Rienecker and Fenton solution at the beginning and at the end of the domain.

We perform simulations with $\frac{N}{\lambda} = 16$ nodes per wavelength and an order $M = 2$ to obtain the steady-state. This order of nonlinearity on the free-surface and on the bottom variation is sufficient to obtain converged results, because the Class I Bragg reflection is second order, as explained in [10]. The local reflection coefficient is then extracted using the method of Suh et al. [15].

The results appear in Fig.4 along with the experimental measurements of [3] and the solution given by the linear perturbation theory of [12]. It appears clearly that our numerical results are very closed to both the linear theory and the experiments. We will now focus on the next test case with a higher bottom variation, to check the ability of the proposed method is able to treat realistic bathymetry profiles with non-negligible variations.

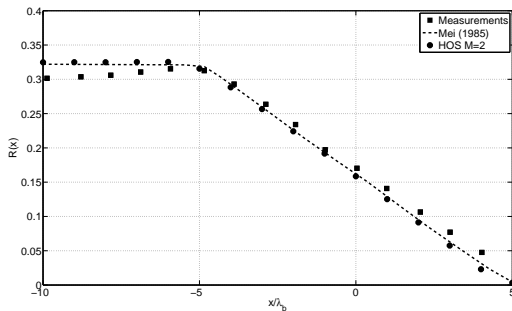


Figure 4: Bragg reflection from a sinusoidal bottom ripple patch over $-5\lambda_b \leq x \leq 5\lambda_b$. $ka = 0.05$ and $k_b d = 0.31$.

Application: harmonic generation over a submerged bar

Here we consider the transformation of non-linear regular waves as they travel up and over a submerged bar. As they propagate over the bar, they steepen and they decompose into higher-frequency free waves, as shown in the experiments [4, 11]. These higher harmonics produce an irregular pattern behind the bar. This validation case is particularly difficult because it requires the accurate propagation of waves in both deep and shallow water. Thus it is often used as a discriminating test case for non-linear models of surface waves propagation over a variable bottom [9, 1]. The bottom variation is defined by

$$\beta(x) = \begin{cases} 0.05(x-6) & \text{for } 6 \leq x \leq 12, \\ 0.3 & \text{for } 12 \leq x \leq 14, \\ 0.3 - 0.1(x-14) & \text{for } 14 \leq x \leq 17, \\ 0 & \text{elsewhere,} \end{cases}$$

and can be seen in Fig.5. It has been scaled with a factor of two in comparison with Dingemans experiments [4].

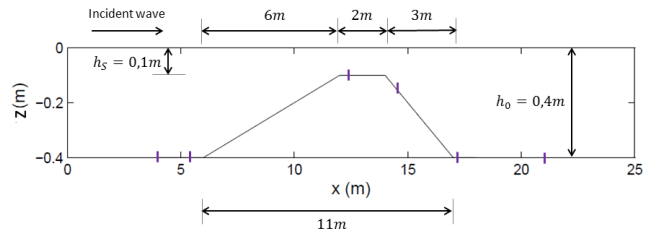


Figure 5: Submerged bar (Dingemans experiments).

Regular waves are generated at the left side of the domain thanks to a solution of Rienecker and Fenton [13] of steepness $ka = 0.0168$ and relative water depth $kh = 0.6725$. The period is fixed to 2.02s with an amplitude of 0.01m.

The convergence and steady-state are reached with 40 nodes per wavelength and an HOS order $M = 17$. Indeed, such a high-order is needed to represent all the nonlinearities induced by the bottom variation.

Time series of surface elevations.

A snapshot of the surface elevation (scaled by a factor of 3) is represented in Fig.6 and the time histories of the surface elevations at various locations are shown in Fig.7. The experimental data comes from the experiment of [11].

The comparison between our numerical results and the experimental data is very good, and similar to the results obtained with other numerical methods [9, 1]. Thus, both free-surface non-linearities and bottom non-linearities are correctly solved and we are confident in the accuracy of the model even for large bottom variations.

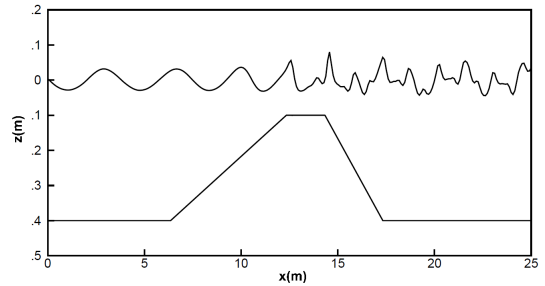


Figure 6: Snapshot of the surface elevation at steady-state.

Harmonic analysis.

For a deeper comparison, an harmonic analysis of the surface elevation is run as presented in [1]. Our results are visible in Fig.8.

As expected, we can clearly observe the generation of high-harmonics over the bar. Moreover, the comparison of all harmonics with the measurements is good even up to the fifth-harmonic. It is also very similar to the numerical results presented in [1], particularly on the slight discrepancies observed on the first harmonic. We can notice that even if $\frac{\beta}{h_0} = 75\%$ over the submerged bar (which represents a very large relative bottom variation), the steepness is weak ($ka = 0.017$), and the bottom variation does not take place on all the domain, so the model is able to solve this problem accurately.

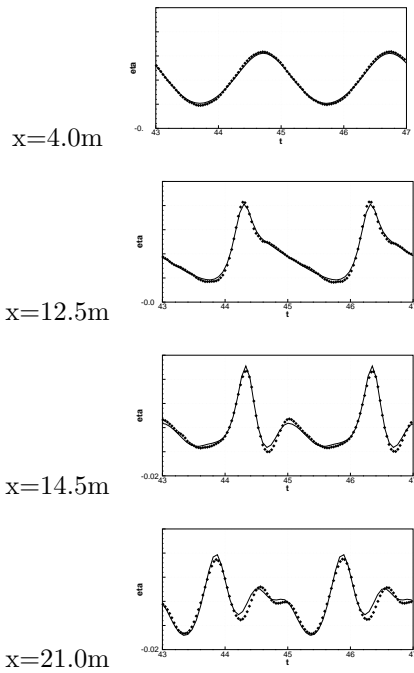


Figure 7: Time series of measured (points) and computed (lines) surface elevations.

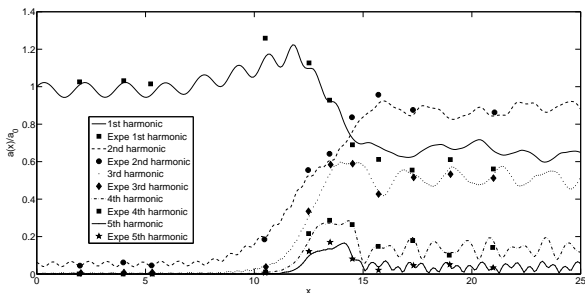


Figure 8: Harmonic analysis. $\frac{N}{\lambda} = 40$ and $M = 17$.

Conclusion

We have implemented a numerical method for the simulation of non-linear free surface waves over variable depth. It is based on a Taylor expansion of the bottom boundary condition with respect to the mean water depth.

A validation case with a constant bottom variation has already been presented in [8] to assess the domain of applicability of our method. By a series of two test cases, we have shown the accuracy of the method for non-constant bottom variations. The first test case reproduces Bragg reflection over small bottom variations and shows results conformed to [10, 1, 9]. The last case simulates highly and realistic varying bottom geometries. It shows very good agreement with both numerical and experimental data, and thus proves the ability of the method to accurately compute high variations of the bathymetry.

The required HOS order is very high for the harmonic generation over a submerged bar, and the bottom and the free-surface do not seem to require expansions with the same order of non-linearity. Thus we will try to improve the method by decoupling the orders of non-linearities

on the free-surface and on the bottom to enhance the efficiency of our model. This has been presented with the DNO method [9, 2], a formalism which exhibits a formalism similar to the HOS method [14].

References

- [1] H.B. Bingham and H. Zhang. On the accuracy of finite-difference solutions for nonlinear water waves. *J. Fluid Mech.*, 58:211–228, 2007.
- [2] Walter Craig, Philippe Guyenne, David P. Nicholls, and Catherine Sulem. Hamiltonian long-wave expansions for water waves over a rough bottom. volume 461, pages 839–873. The Royal Society, 2005.
- [3] A. G. Davies and A. D. Heathershaw. Surface-wave propagation over sinusoidally varying topography. *Journal of Fluid Mechanics*, 144:419–443, 7 1984.
- [4] M.W. Dingemans. Comparison of computations with Boussinesq-like models and laboratory measurements. *Delft Hydraulics memo H1684.12.*, 1994.
- [5] D.G. Dommermuth and D.K.P. Yue. A high-order spectral method for the study of non-linear gravity waves. *J. Fluid Mech.*, 184:267–288, 1986.
- [6] G. Ducrozet, F. Bonnefoy, D. Le Touzé, and P. Ferrant. 3-D HOS simulations of extreme waves in open seas. *Nat. Hazards Earth Syst. Sci.*, 7:109–122, 2007.
- [7] G. Ducrozet, F. Bonnefoy, D. Le Touze, and P. Ferrant. A modified high-order spectral method for wavemaker modeling in a numerical wave tank. *Eur. J Mech. B, Fluid.*, 34:19–34, 2012.
- [8] M. Gouin, G. Ducrozet, and P. Ferrant. Development of a highly nonlinear model for wave propagation over a variable bathymetry. In *26th international workshop on water waves and floating bodies, Proceedings*, 2014.
- [9] P. Guyenne and D.P. Nicholls. A high-order spectral method for nonlinear water waves over moving bottom topography. *J. Sci. Comput.*, 30:81–101, 2007.
- [10] Y. Liu and D.K.P. Yue. On generalized Bragg scattering of surface waves by bottom ripples. *J. Fluid Mech.*, 356:297–326, 1998.
- [11] H.R. Luth, G. Klopman, and N. Kitou. Kinematics of waves breaking partially on an offshore bar. *Delft Hydraulics memo H1573*, 1994.
- [12] Chiang C. Mei. Resonant reflection of surface water waves by periodic sandbars. *J. Fluid Mech.*, 152:315–335, 1985.
- [13] M.M. Rienecker and J.D. Fenton. A Fourier approximation method for steady water waves. *J. Fluid Mech.*, 104:119–137, 1981.
- [14] H.A. Schaffer. Comparison of Dirichlet-Neumann operator expansions for nonlinear surface gravity waves. *Coast. Engng.*, 55(4):288–294, 2008.
- [15] Kyung Doug Suh, Woo Sun Park, and Beom Seok Park. Separation of incident and reflected waves in wavecurrent flumes. *Coastal Engineering*, 43(34):149–159, 2001.
- [16] B.J. West, K.A. Brueckner, R. S. Janda, D. M. Milder, and R. L. Milton. A new numerical method for the surface hydrodynamics. *J. Geophys. Res.*, 92:11803–11824, 1987.